NANO LETTERS

pubs.acs.org/NanoLett Letter

Pressure-Driven Solid-State Radical Polymerization toward Carbon Nanothread

Guangwei Che,[▽] Xingyu Tang,[▽] Jie Liu, Puyi Lang, Yunfan Fei, Xin Yang, Yajie Wang, Dexiang Gao, Xiaoge Wang, Jing Ju, Aijiao Guan, Junfeng Xiang, Xiao Dong, Takanori Hattori, Jun Abe, Haiyan Zheng, and Kuo Li*

Cite This: https://doi.org/10.1021/acs.nanolett.5c03977 Read Online

ACCESS | Metrics & More | Article Recommendations | Supporting Information

ABSTRACT: Mechanochemical radical polymerization has unique advantages in the synthesis of polymers due to its reduced solvent consumption and adaptability of insoluble monomers. However, it suffers from the uncontrollable degradation of the formed polymers during reaction, and a new synthetic strategy with precise controllability needs to be developed. Here, by employing high static pressure up to 30 GPa, we found 1,3,5-trifluorobenzene undergoes radical polymerization by breaking the conjugated π-bonds and forms a carbon nanothread with high selectivity (Polymer-I polymorph). Based on the crystal structure at the threshold pressure and the calculated energy barriers for the bonding pathway, we concluded that the benzene rings react via a radical 1,2-addition pathway. Our work highlights that high pressure is a robust method to initiate solid-state radical polymerization, even for very stable aromatics, and offers fresh insights for the synthesis of polymeric carbon-based materials with high selectivity.

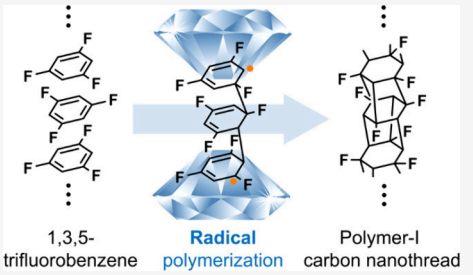

KEYWORDS: *Solid-State Radical Polymerization, Polymer-I Carbon Nanothread, 1,3,5-Trifluorobenzene, High Pressure*

Solid-state radical polymerization receives increasing attention due to its inherent advantages, including the reduction of solvent consumption, application to the nonsoluble monomer, and the avoidance of reaction termination caused by fast precipitation.[1] The typical methods to initiate the solid-state radical polymerization include radiation-initiation, frontal polymerization strategy, and mechanochemical synthesis.[2−5] Among them, recently, mechanochemical synthesis is growing fast in use, and it can construct one- to three-dimensional polymers via shearing, grinding by using the mortar-and-pestle, high-speed ball milling, and reactive extrusion. Recently, a novel piezocatalysis synthesis method striking with a hammer was reported to obtain the cross-linking polymer by radical polymerization.[6] Despite the rapid expansion of mechanochemistry synthesis, a distinct disadvantage of the mechanochemical polymerization has impeded its development, that is, the uncontrollable degradation of the newly formed polymer when increasing the reaction time or changing the milling parameters.[1,7,8] Moreover, the shearing and compression produced by the mortar-and-pestle, high-speed ball milling, and hammer cannot be quantified. Therefore, the reaction mechanism at molecular levels remained "a black box", and reproducibly it always depends on the equipment.

Static high pressure can continuously and quantitatively tune the intermolecular distance,[9−11] which is a precise and robust tool for solid-state mechanochemical synthesis. One of the most famous polymeric carbon materials synthesized is carbon nanothread (CNTh),[12,13] which was predicted to possess exceptional strength, tenacity, and a tunable band gap and can only be synthesized via high-pressure polymerization of aromatics.[14,15] Up to now, the most possible reaction path of this solid-state polymerization was concluded as [4 + 2] cycloaddition,[16] including the polymerization of pyridine,[17] aniline,[18] furan,[19] thiophene,[20] 2,5-furandicarboxylic acid,[21] and pyridazine[22] as well as naphthalene/octafluoronaphthalene[23] and anthracene/octafluoronaphthalene.[24] In this work, we found, under static compression, 1,3,5-trifluorobenzene (1,3,5-TFB) polymerized via a radical reaction by breaking the conjugated π-bonds. The reaction produced CNTh with an unprecedented Polymer-I structure characterized by five-membered rings. This CNTh was predicted to exhibit superior torsional deformation capacity and enhanced interfacial load-transfer efficiency,[25] as well as the largest bandgap of 4.79 eV among CNThs,[14] thereby holding potential application in nanofiber[25] and energy storage devices.[26] Our findings highlight a new and promising method to initiate the π-electron radical polymerization of aromatic compounds and

Received: August 1, 2025
Revised: August 30, 2025
Accepted: September 15, 2025

offer new insights into the reaction mechanism of the aromatics besides the well-known aromatic substitution reaction at ambient pressure and addition reaction at high pressure.[16]

Transparent liquid 1,3,5-TFB was cryogenically loaded into a Paris−Edinburgh press using a liquid nitrogen bath and compressed to 30.0 GPa. After decompression, a white solid product (PE-30) was obtained. Selected area electron diffraction (SAED) of PE-30 was shown in Figure 1a.

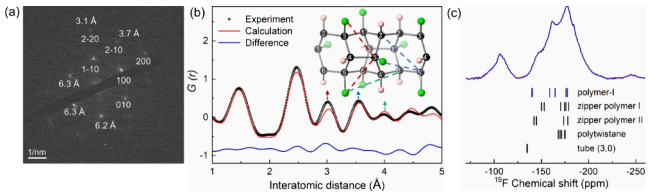

Figure 1. Investigations of inter- and intrathread structures of PE-30. (a) Selected area electron diffraction (SAED) of PE-30. (b) X-ray PDF refinement plot for experimental data of PE-30 and the Polymer-I CNTh using PDFgui2 with R_w = 0.191. The inset shows the distances of atom pairs in the Polymer-I CNTh model, corresponding to the peaks in the $G(r)$ pattern. (c) ^{19}F ssNMR of the PE-30 and simulated results of the CNTh models. Vertical bars represent the simulated chemical shifts of CNTh models.

Diffraction peaks at 6.3, 3.7, and 3.1 Å were observed and indexed as {010}, {110}, and {020}, respectively, using a hexagonal lattice with a = 7.3 Å, which is the feature of CNTh.[12,13,27] As many CNThs only show the first-order diffraction, PE-30 has a better crystallinity.[13,17,19] X-ray diffraction (XRD) of PE-30 was also performed, which revealed a diffraction peak at d = 6.3 Å, as shown in Supporting Information Figure S1.

To investigate the intrathread structure of PE-30, the X-ray pair distribution function (PDF) and ^{19}F solid-state nuclear magnetic resonance (ssNMR) were investigated. We performed PDF refinement using all typical intrathread structures (Figure S2a) and found that only Polymer-I fit the experimental data well (Figure 1b), while the others showed significant deviations, as illustrated in Figure S2b. As shown in Figure 1b, the first peak at 1.50 Å represents the sp^3 C−C and C−F bonds in CNTh. The peak at 2.45 Å corresponds to the meta-position C−C pair of a hexagonal carbon ring of CNTh. Most importantly, the peak at r = 3.02 Å is related to the meta-position C−F pair of the five-membered ring (marked with a red dotted line in Figure 1b), which is characteristic of Polymer-I CNTh. The peaks at r = 3.57 and 4.00 Å correspond to the distances between C2′−C5″, F3′−C5″ (marked in blue dotted line in Figure 1b) and F5−C6″, respectively (marked in green dotted line in Figure 1b).

^{19}F magic angle spinning (MAS) ssNMR was collected as shown in Figure 1c. Three broad peaks centered at −179, −162, and −147 ppm are ascribed to the fluorine atoms connected with C(sp^3) (F−CR$_3$), and the peak at −109 ppm corresponds to the F atom in C(-H)=C(-F). The chemical shift simulations of ^{19}F ssNMR for models are highlighted by vertical bars. Clearly, Polymer-I was identified by comparing the experimental NMR data with the simulated results. The ^{1}H−^{13}C cross-polarization (CP) ^{1}H decoupling ssNMR is also consistent with the simulated chemical shifts of Polymer-I as shown in Figure S3, which demonstrated Polymer-I CNTh again.

Polymer-I contains two edge-shared five-membered rings between the phenyl units, which requires a distinctive reaction other than the Diel-Alder reaction, etc. Chen et al. suggests that the para-polymerization which includes the reactive radicals is also a potential reaction mechanism leading to the nanothread with Polymer-I structure.[16] We performed the electron paramagnetic resonance (EPR) of PE-30 to probe radicals. To prevent the radicals from being eliminated by oxygen, the synthesis of PE-30 and the loading into EPR cell were all performed in an Ar-filled glovebox, and the EPR spectrum is shown in Figure 2. Two main peaks with line

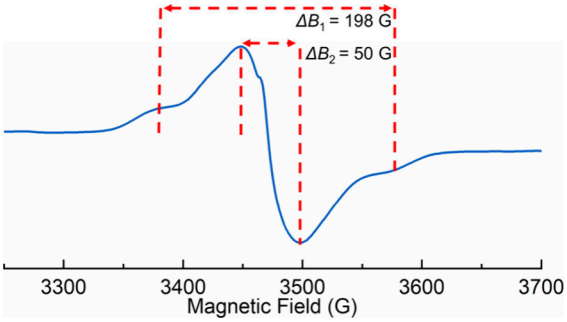

Figure 2. EPR spectra of PE-30. The data were collected in Ar atmosphere.

widths (ΔB) of 50 and 198 G were observed, and the signal with ΔB_1 = 198 G was identified as F-substituted carbon radicals based on the literature,[28] which clearly demonstrated the evolvement of free radical in the synthesis of PE-30.

To find the radical polymerization reaction route from 1,3,5-TFB, we extracted the oligomers by n-hexane (C_6H_{14}) from PE-30 and performed the gas chromatography mass spectrometry (GC-MS) (Figure 3). To avoid interference, we synthesized and unpacked the sample in Ar. As shown in Figure 3a, three groups of oligomers with the abundance of each oligomer > 0.19% were distinguished, and parts of them were identified by comparing the mass spectra to the reported oligomers in ref 29 and by searching the National Institute of Standards and Technology/Wiley standard library, as shown in Figures S4 and S5.

The first group (including $C_{10}H_4F_4$ and $C_{18}H_9F_9$) and the second group ($C_{12}H_5F_5$, $C_{12}H_4F_6$, $C_{12}H_6F_4$, $C_{18}H_6F_8$ and $C_{18}H_7F_7$) were recognized to be formed via [4 + 2] reaction and 1,1′-coupling,[29] respectively (Figures S4 and S6). The third group includes $C_{12}H_5F_5'$ (two isomers) and $C_{18}H_8F_8$ (16 isomers). Their mass spectra show a strong molecular ion peak and strong $C_{12}H_4F_4^+$ and $C_{10}H_4F_4^+$ fragments (Figure 3b), which are distinguished from the others (Figure S4). They mostly transformed to $C_{12}H_5OF_5$ and $C_{18}H_8OF_8$ when synthesized and opened in air. Therefore, they are regarded as free-radical moieties, consistent with the EPR results. We then investigated the quantities of these three groups to evaluate the contribution of the three polymerization paths in the formation of CNTh. As shown in Figure 3a, in the first group, the trimer $C_{18}H_9F_9$ has a content of 0.39%, much lower than that of the dimers $C_{10}H_4F_4$ (8.21%); in the second group, the trimers have a content of 5.58%, also much lower than that of the dimers (53.96%). These indicate that both the [4 + 2] reaction and 1,1′-coupling were suppressed in the polymerization to a higher degree. In contrast, in the third group, the content of trimers is much higher than that of dimers (18.86%

https://doi.org/10.1021/acs.nanolett.5c03977
Nano Lett. XXXX, XXX, XXX−XXX

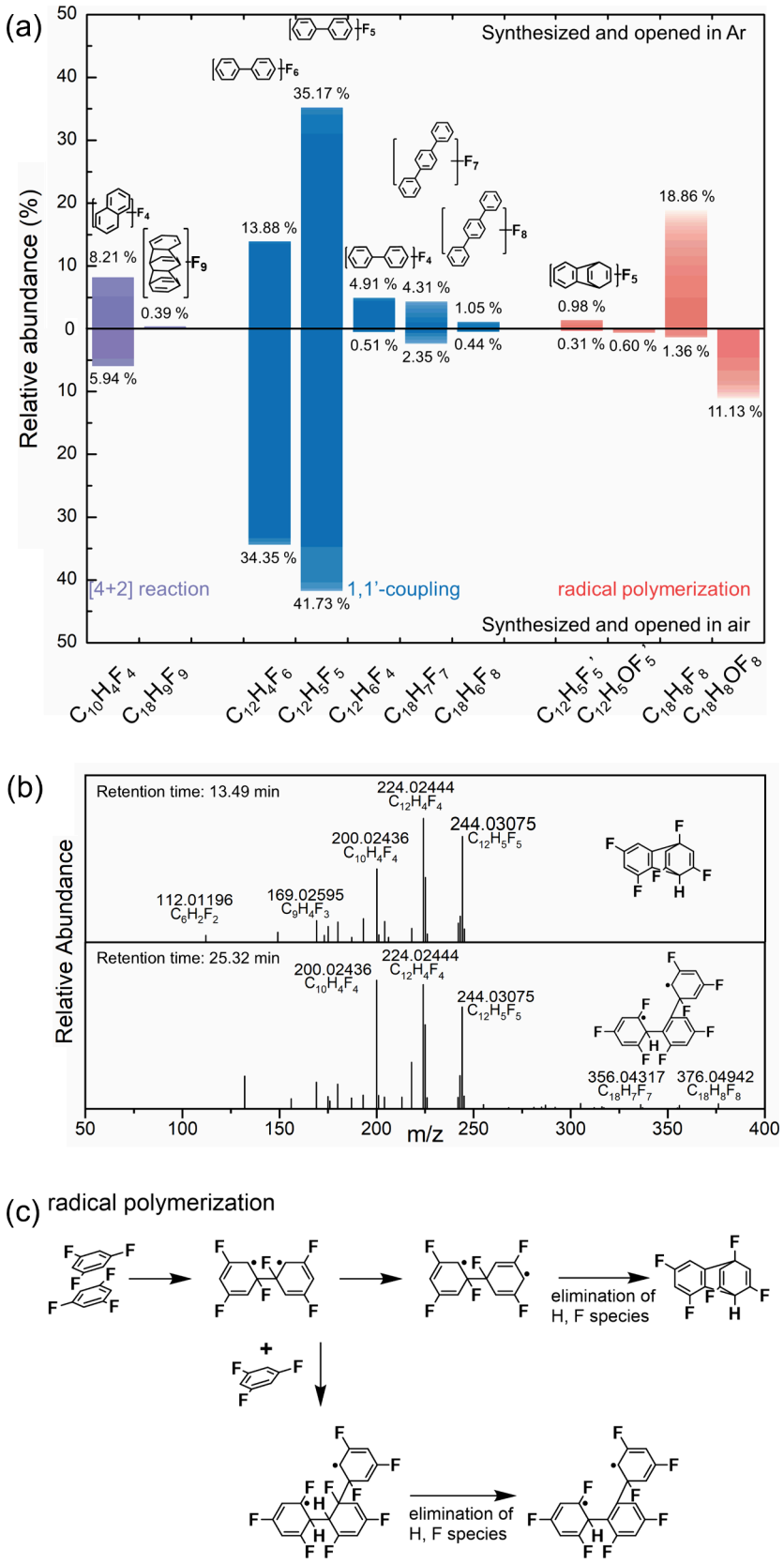

Figure 3. Evidence of radical polymerization. (a) Content variation of oligomers of [4 + 2] reaction, 1,1′-coupling reaction, and radical polymerization, as the degree of polymerization increases. Measured PE-30 was synthesized and open in Ar and air for top and bottom plots, respectively. (b) Mass spectra of $C_{12}H_5F_5'$ and $C_{18}H_8F_8$. (c) Proposed radical polymerization reaction of 1,3,5-TFB under high pressure.

for $C_{18}H_8F_8$ vs 0.98% for $C_{12}H_5F_5'$). It indicates that 1,3,5-TFB follows this radical reaction to form Polymer-I CNTh.

The mass spectra of two isomers of $C_{12}H_5F_5'$ in the third group are almost identical (Figure S5a). Referring to the NIST

https://doi.org/10.1021/acs.nanolett.5c03977
Nano Lett. XXXX, XXX, XXX−XXX

database, they can be identified as F-substituted 1,4-etheno-1,4-dihydronaphthalene or similar structures (Figure S5b). For $C_{18}H_8F_8$ (16 isomers exhibit similar mass spectra, Figure 3b bottom), its dimeric fragments of $C_{12}H_5F_5^+$, $C_{12}H_4F_4^+$, and $C_{10}H_4F_4^+$ are similar to those of $C_{12}H_5F_5'$, which indicates it is a fragile addition product between $C_{12}H_5F_5'$ and $C_6H_3F_3$ (the corresponding fragmentation mechanism is presented in Figure S7). Based on the above discussion, a radical polymerization reaction was proposed as shown in Figure 3c, corresponding to theoretical calculations as mentioned later.

The threshold structure is the basis for a theoretical investigation of the reaction mechanism. We conducted an in situ neutron diffraction experiment (Figure S8), and a phase transition at 2.0 GPa was demonstrated in accord with results of in situ Raman and IR spectroscopy (Figures S9 and S10, Tables S1 and S2). The crystal structures of phase I at 1.0 GPa and phase II at 4.0 GPa were both determined by Rietveld refinement, as shown in Figure S11, with atomic coordinates in Tables S3 and S4. We also refined the neutron diffraction data collected at higher pressure (Figure S12 and Table S5) and obtained the equation of state (EOS, Figure S13). The threshold structure at 20.0 GPa was then determined by geometry optimization using DFT (Figure 4a), at which

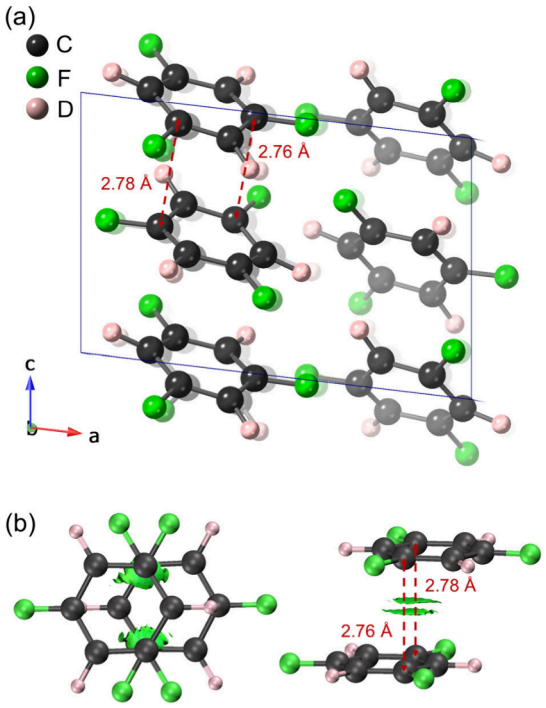

Figure 4. Investigation of the threshold structure at 20.0 GPa. (a) Threshold structure at 20.0 GPa. (b) Weak interaction analysis of threshold structure at 20.0 GPa.

pressure the reaction is going to occur, as determined by in situ Raman and IR in Figures S9 and S10. The volume of the obtained lattice is supported by the EOS, and the atomic coordinates are shown in Table S6. Within the threshold structure, molecules exhibit inclined columnar stacking and Gaussian software was used to perform a weak interaction analysis between them. As shown in Figure 4b, prominent interactions between meta-position C(F) atoms in adjacent molecules were identified, with the closest intermolecular distances of 2.76 and 2.78 Å. This indicates the polymerization likely starts from the bonding between the C(F) atoms.[9−11,29]

To clarify the mechanism of unprecedented high-pressure radical reaction, theoretical calculations using the nudged elastic band (NEB) method were conducted to investigate the reaction process from 1,3,5-TFB to Polymer-I at 20.0 GPa. A single-column model extracted from the threshold model (20.0 GPa), containing two repeating units (4 molecules) along the packing direction, was adopted. A possible reaction pathway was explored, of which the thermodynamically most reasonable path was illustrated in Figure 5. The consecutive 1,2-addition

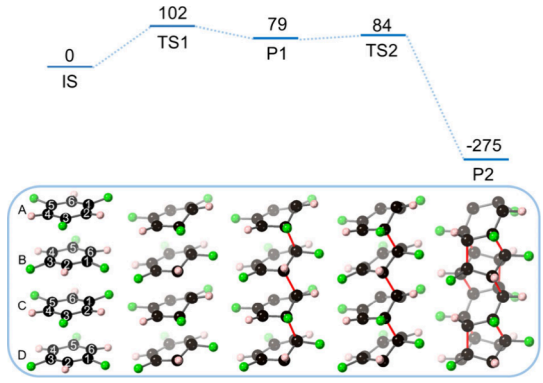

Figure 5. Thermodynamically reasonable reaction process. Key structures along the path with its relative enthalpy values (kJ/mol) were displayed. The molecules and carbon atoms were denoted to better describe the bonding process.

reactions occurred first as the key step with an energy barrier of 102 kJ/mol $C_6F_3H_3$. Bonds were formed between C_{A3} and C_{B1} (carbon 3 in molecule A and carbon 1 in molecule B as shown in Figure 5), C_{B2} and C_{C2}, and C_{C3} and C_{D1}, respectively, forming 1,2-addition product (P1). This is consistent with the oligomers $C_{18}H_8F_8$ observed in GC-MS, providing a possible explanation for this unprecedented radical polymerization. The 1,2-addition product (P1) was unstable, making it susceptible to further polymerization. Surprisingly, C_{B4} and C_{C6} became more reactive in the subsequent polymerization process (Figure S14), leading to Polymer-I CNTh. In contrast to nonpolar 1,3,5-trifluorobenzene, 1,2,3-trifluorobenzene exhibits a strong dipole moment and columnar antiparallel $\pi\cdots\pi$ stacking.[30] Therefore, it polymerized via selective sequential [4 + 2] polymerization between H-carbon dienophile/F-carbon dienophile and F, H-carbon diene within the column, followed by the "zippered" bonding of the remaining atoms, leading to zipper polymer CNTh. The difference in reaction pathways stems from the distinct substitution patterns of the fluorine atoms, which not only influence the molecular charge distribution—thereby modulating molecular packing—but also regulate the reactivity of carbon atoms in the aromatic ring.

In summary, by compressing 1,3,5-TFB with electron-withdrawing fluorine (F) atoms distributed in the meta-position to 30 GPa, we synthesized a hexagonally stacked Polymer-I CNTh, which was determined by SAED, XRD, PDF, and NMR. The pressure-induced polymerization (PIP) of 1,3,5-TFB is radical polymerization as disclosed by the GC-MS and EPR spectra of PE-30. By investigating the energy barrier, we conclude that the 1,2-addition reaction is the reaction route. Our work evidences a new reaction mechanism of aromatics experimentally, parallel to the aromatic sub-

https://doi.org/10.1021/acs.nanolett.5c03977
Nano Lett. XXXX, XXX, XXX−XXX

stitution reaction at ambient pressure, and the [4 + 2] reaction happened at high pressure. More importantly, we highlight that static high pressure can offer a controllable pathway to generate a radical for the initiation of solid-state polymerization.

■ ASSOCIATED CONTENT

Supporting Information

The Supporting Information is available free of charge at https://pubs.acs.org/doi/10.1021/acs.nanolett.5c03977.

Experimental procedures including synthesis of product and in situ Raman, IR, and neutron diffraction measurements; EPR, XRD, SAED, and PDF measurements; geometry optimization of structures; product models; calculations of IR, Raman, and NMR spectra; vc-NEB calculations; noncovalent intermolecular interaction analysis (PDF)

■ AUTHOR INFORMATION

Corresponding Author

Kuo Li − *Center for High Pressure Science and Technology Advanced Research, Beijing 100193, P. R. China;* orcid.org/0000-0002-4859-6099; Email: likuo@hpstar.ac.cn

Authors

Guangwei Che − *Center for High Pressure Science and Technology Advanced Research, Beijing 100193, P. R. China*

Xingyu Tang − *Center for High Pressure Science and Technology Advanced Research, Beijing 100193, P. R. China*

Jie Liu − *Center for High Pressure Science and Technology Advanced Research, Beijing 100193, P. R. China*

Puyi Lang − *Center for High Pressure Science and Technology Advanced Research, Beijing 100193, P. R. China*

Yunfan Fei − *Center for High Pressure Science and Technology Advanced Research, Beijing 100193, P. R. China*

Xin Yang − *Center for High Pressure Science and Technology Advanced Research, Beijing 100193, P. R. China*

Yajie Wang − *Center for High Pressure Science and Technology Advanced Research, Beijing 100193, P. R. China*

Dexiang Gao − *Center for High Pressure Science and Technology Advanced Research, Beijing 100193, P. R. China*

Xiaoge Wang − *College of Chemistry and Molecular Engineering, Peking University, Beijing 100871, P. R. China*

Jing Ju − *College of Chemistry and Molecular Engineering, Peking University, Beijing 100871, P. R. China;* orcid.org/0000-0001-9540-2165

Aijiao Guan − *Institute of Chemistry, Chinese Academy of Science, Beijing 100190, P. R. China*

Junfeng Xiang − *Institute of Chemistry, Chinese Academy of Science, Beijing 100190, P. R. China*

Xiao Dong − *Key Laboratory of Weak-Light Nonlinear Photonics School of Physics, Nankai University, Tianjin 300071, P. R. China;* orcid.org/0000-0003-4533-1914

Takanori Hattori − *J-PARC Center, Japan Atomic Energy Agency, Tokai, Ibaraki 319-1195, Japan*

Jun Abe − *Neutron Science and Technology Center, Comprehensive Research Organization for Science and Society, Tokai, Ibaraki 319-1106, Japan*

Haiyan Zheng − *Center for High Pressure Science and Technology Advanced Research, Beijing 100193, P. R. China;* orcid.org/0000-0002-4727-5912

Complete contact information is available at: https://pubs.acs.org/10.1021/acs.nanolett.5c03977

Author Contributions

[▽]G.C. and X.T. contributed equally to this work.

Notes

The authors declare no competing financial interest.

■ ACKNOWLEDGMENTS

The authors acknowledge the support of the National Key Research and Development Program of China (2023YFA1406200). The authors also acknowledge the support of the National Natural Science Foundation of China (Grant No. 22022101). This work was carried out with the support of BL13HB1 at the Shanghai Synchrotron Radiation Facility. In situ neutron diffraction experiment at the Materials and Life Science Experimental Facility in J-PARC was performed through a user program (Proposal No. 2023B0100). This study was also partially supported by Synergetic Extreme Condition User Facility (SECUF).

■ ABBREVIATIONS

1,3,5-TFB, 1,3,5-trifluorobenzene; CNTh, carbon nanothread; CP, cross-polarization; DFT, density functional theory; EPR, electron paramagnetic resonance; GC-MS, gas chromatography mass spectrometry; MAS, magic angle spinning; NEB, nudged elastic band; PDF, pair distribution function; PE-30, product synthesized by Paris−Edinburgh press at 30.0 GPa; SAED, selected area electron diffraction; ssNMR, solid-state nuclear magnetic resonance; XRD, X-ray diffraction

■ REFERENCES

(1) Krusenbaum, A.; Grätz, S.; Tigineh, G. T.; Borchardt, L.; Kim, J. G. The Mechanochemical Synthesis of Polymers. *Chem. Soc. Rev.* **2022**, *51*, 2873.

(2) Adler, G.; Ballantine, D.; Baysal, B. The Mechanism of Free Radical Polymerization in the Solid State. *J. Polym. Sci.* **1960**, *48*, 195−206.

(3) Mel'nikov, M. Y.; Fok, N. V. Photochemical Reactions of Free Radicals in the Solid Phase. *Russ. Chem. Rev.* **1980**, *49*, 131−142.

(4) Cho, H. Y.; Bielawski, C. W. Atom Transfer Radical Polymerization in the Solid-State. *Angew. Chem., Int. Ed.* **2020**, *59*, 13929−13935.

(5) Robertson, I. D.; Yourdkhani, M.; Centellas, P. J.; Aw, J. E.; Ivanoff, D. G.; Goli, E.; Lloyd, E. M.; Dean, L. M.; Sottos, N. R.; Geubelle, P. H.; Moore, J. S.; White, S. R. Rapid Energy-Efficient Manufacturing of Polymers and Composites via Frontal Polymerization. *Nature* **2018**, *557*, 223−227.

(6) Nothling, M. D.; Daniels, J. E.; Vo, Y.; Johan, I.; Stenzel, M. H. Mechanically Activated Solid-State Radical Polymerization and Cross-Linking via Piezocatalysis. *Angew. Chem., Int. Ed.* **2023**, *62*, No. e202218955.

(7) Caruso, M. M.; Davis, D. A.; Shen, Q.; Odom, S. A.; Sottos, N. R.; White, S. R.; Moore, J. S. Mechanically-Induced Chemical Changes in Polymeric Materials. *Chem. Rev.* **2009**, *109*, 5755.

(8) Kondo, S.; Sasai, Y.; Hosaka, S.; Ishikawa, T.; Kuzuya, M. Kinetic Analysis of the Mechanolysis of Polymethylmethacrylate in the Course of Vibratory Ball Milling at Various Mechanical Energy. *J. Polym. Sci. Part A* **2004**, *42*, 4161.

(9) Zhao, W.; Zhang, J.; Sun, Z.; Xiao, G.; Zheng, H.; Li, K.; Li, M.-R.; Zou, B. Chemical Synthesis Driven by High Pressure. *CCS Chem.* **2025**, *7*, 1250−1271.

(10) Tang, X.; Dong, X.; Zhang, C.; Li, K.; Zheng, H.; Mao, H.-k. Triggering Dynamics of Acetylene Topochemical Polymerization. *Matter Radiat. Extremes* **2023**, *8*, 058402.

(11) Fei, Y.; Li, K.; Zheng, H. Synthesis of Nano-Carbon Materials by High Pressure Solid-State Topochemical Polymerization. *Chin. J. High Press. Phys.* **2023**, *37*, 060101.
(12) Fitzgibbons, T. C.; Guthrie, M.; Xu, E. S.; Crespi, V. H.; Davidowski, S. K.; Cody, G. D.; Alem, N.; Badding, J. V. Benzene-Derived Carbon Nanothreads. *Nat. Mater.* **2015**, *14*, 43−47.
(13) Li, X.; Baldini, M.; Wang, T.; Chen, B.; Xu, E.; Vermilyea, B.; Crespi, V. H.; Hoffmann, R.; Molaison, J. J.; Tulk, C. A.; Guthrie, M.; Sinogeikin, S.; Badding, J. V. Mechanochemical Synthesis of Carbon Nanothread Single Crystals. *J. Am. Chem. Soc.* **2017**, *139*, 16343−16349.
(14) Xu, E.-s.; Lammert, P. E.; Crespi, V. H. Systematic Enumeration of sp^3 Nanothreads. *Nano Lett.* **2015**, *15*, 5124−5130.
(15) Roman, R. E.; Kwan, K.; Cranford, S. W. Mechanical Properties and Defect Sensitivity of Diamond Nanothreads. *Nano Lett.* **2015**, *15*, 1585−1590.
(16) Chen, B.; Hoffmann, R.; Ashcroft, N. W.; Badding, J.; Xu, E.; Crespi, V. Linearly Polymerized Benzene Arrays as Intermediates, Tracing Pathways to Carbon Nanothreads. *J. Am. Chem. Soc.* **2015**, *137*, 14373−14386.
(17) Li, X.; Wang, T.; Duan, P.; Baldini, M.; Huang, H.-T.; Chen, B.; Juhl, S. J.; Koeplinger, D.; Crespi, V. H.; Schmidt-Rohr, K.; Hoffmann, R.; Alem, N.; Guthrie, M.; Zhang, X.; Badding, J. V. Carbon Nitride Nanothread Crystals Derived from Pyridine. *J. Am. Chem. Soc.* **2018**, *140*, 4969−4972.
(18) Nobrega, M. M.; Teixeira-Neto, E.; Cairns, A. B.; Temperini, M. L. A.; Bini, R. One-dimensional Diamondoid Polyaniline-like Nanothreads from Compressed Crystal Aniline. *Chem. Sci.* **2018**, *9*, 254−260.
(19) Huss, S.; Wu, S.; Chen, B.; Wang, T.; Gerthoffer, M. C.; Ryan, D. J.; Smith, S. E.; Crespi, V. H.; Badding, J. V.; Elacqua, E. Scalable Synthesis of Crystalline One-Dimensional Carbon Nanothreads through Modest-Pressure Polymerization of Furan. *ACS Nano* **2021**, *15*, 4134−4143.
(20) Biswas, A.; Ward, M. D.; Wang, T.; Zhu, L.; Huang, H.-T.; Badding, J. V.; Crespi, V. H.; Strobel, T. A. Evidence for Orientational Order in Nanothreads Derived from Thiophene. *J. Phys. Chem. Lett.* **2019**, *10*, 7164−7171.
(21) Wang, X.; Yang, X.; Wang, Y.; Tang, X.; Zheng, H.; Zhang, P.; Gao, D.; Che, G.; Wang, Z.; Guan, A.; Xiang, J.-F.; Tang, M.; Dong, X.; Li, K.; Mao, H.-k. From Biomass to Functional Crystalline Diamond Nanothread: Pressure-Induced Polymerization of 2,5-Furandicarboxylic Acid. *J. Am. Chem. Soc.* **2022**, *144*, 21837−21842.
(22) Dunning, S. G.; Zhu, L.; Chen, B.; Chariton, S.; Prakapenka, V. B.; Somayazulu, M.; Strobel, T. A. Solid-State Pathway Control via Reaction-Directing Heteroatoms: Ordered Pyridazine Nanothreads through Selective Cycloaddition. *J. Am. Chem. Soc.* **2022**, *144*, 2073−2078.
(23) Ward, M. D.; Tang, W. S.; Zhu, L.; Popov, D.; Cody, G. D.; Strobel, T. A. Controlled Single-Crystalline Polymerization of $C_{10}H_8$·$C_{10}F_8$ under Pressure. *Macromolecules* **2019**, *52*, 7557−7563.
(24) Friedrich, A.; Collings, I. E.; Dziubek, K. F.; Fanetti, S.; Radacki, K.; Ruiz-Fuertes, J.; Pellicer-Porres, J.; Hanfland, M.; Sieh, D.; Bini, R.; Clark, S. J.; Marder, T. B. Pressure-Induced Polymerization of Polycyclic Arene-Perfluoroarene Cocrystals: Single Crystal X-ray Diffraction Studies, Reaction Kinetics, and Design of Columnar Hydrofluorocarbons. *J. Am. Chem. Soc.* **2020**, *142*, 18907−18923.
(25) Zhan, H.; Zhang, G.; Tan, V. B. C.; Gu, Y. The Best Features of Diamond Nanothread for Nanofibre Applications. *Nat. Commun.* **2017**, *8*, 14863.
(26) Zhan, H.; Zhang, G.; Bell, J. M.; Tan, V. B. C.; Gu, Y. High Density Mechanical Energy Storage with Carbon Nanothread Bundle. *Nat. Commun.* **2020**, *11*, 1905.
(27) Gao, D.; Tang, X.; Xu, J.; Yang, X.; Zhang, P.; Che, G.; Wang, Y.; Chen, Y.; Gao, X.; Dong, X.; Zheng, H.; Li, K.; Mao, H.-k. Crystalline $C_3N_3H_3$ Tube (3,0) Nanothreads. *Proc. Natl. Acad. Sci. U. S. A.* **2022**, *119*, No. e2201165119.
(28) Siegel, S.; Hedgpeth, H. Chemistry of Irradiation Induced Polytetrafiuoroethylene Radicals: I. Re-examination of the EPR Spectra. *J. Chem. Phys.* **1967**, *46*, 3904−3912.
(29) Wang, Y.; Dong, X.; Tang, X.; Zheng, H.; Li, K.; Lin, X.; Fang, L.; Sun, G.; Chen, X.; Xie, L.; Bull, C. L.; Funnell, N. P.; Hattori, T.; Sano-Furukawa, A.; Chen, J.; Hensley, D. K.; Cody, G.; Ren, Y.; Lee, H. H.; Mao, H-k. Pressure-Induced Diels-Alder Reactions in C_6H_6-C_6F_6 Cocrystal towards Graphane Structure. *Angew. Chem., Int. Ed.* **2019**, *58*, 1468−1473.
(30) Che, G.; Tang, X.; Lang, P.; Liu, J.; Wang, Y.; Wang, X.; Wang, X.; Ju, J.; Guan, A.; Li, Q.; Xiang, J.; Guo, L.; Qiao, Y.; Dong, X.; Mao, H.-k.; Zheng, H.; Li, K. Fluorine-Directed Structure-Specific Carbon Nanothreads. *Chem.—Eur. J.* **2025**, *31*, No. e202501735.

https://doi.org/10.1021/acs.nanolett.5c03977
Nano Lett. XXXX, XXX, XXX−XXX